Theoretical Study of ^{31}P NMR Chemical Shifts for Organophosphorus Esters, Their Anions and *O,O*-Dimethylthiophosphorate Anion with Metal Complexes

In Sun Koo,[†,‡,*,a] Dildar Ali,[†,b] Kiyull Yang,[‡] Yong Park,[†,*] David M. Wardlaw,[§] and Erwin Buncel[†]

[†]*Department of Chemistry, Queen's University, Kingston, ON, K7L 3N6, Canada*
[‡]*Department of Chemistry Education and Research Institute of Natural Science, Gyeongsang National University, Jinju, Gyeongnam 660-701, Korea.* [*]*E-mail: iskoo@gnu.ac.kr*
[§]*Faculty of Science, University of Western Ontario, London, ON, N6A 3K7, Canada*
Received September 4, 2008

Ab initio and density functional theory (DFT) studies along with gauge-including atomic orbitals (GIAO) have been carried out on ^{31}P NMR chemical shifts for a series of organophosphorus esters, replacing (RO)P=O by (RS)P=O, (RO)P=S and (RS)P=S functionalities, and for *O,O*-dimethylthiophosphorate ion (PA$^-$) complexed with metal ions (Ag$^+$, Hg^{2+}). *Ab initio* and DFT results are in good agreement with experimental ^{31}P NMR chemical shifts. It is shown that the major contribution of ^{31}P NMR chemical shifts derives from the total paramagnetic tensor and variation of d orbital population at P atom by d_π-p_π bond back-donation.

**Key Word:** ^{31}P NMR chemical shift, Density functional theory (DFT), Diamagnetic and paramagnetic tensor, d_π-p_π bond back-donation

Introduction

^{31}P NMR as a structural tool for identification in the field of organophosphorus chemistry is srongly influenced through the sensitivity of the ^{31}P NMR chemical shift to the structural environment.[1] In turn, ^{31}P shifts provide valuable information about the nearest neighbors of the P atom in the molecule.[2] To illustrate, interestingly, a literature survey showed that the ^{31}P NMR chemical shifts of structurally modified OP ester pesticides, replacing (RO)P=O by (RS)P=O, (RO)P=S and (RS)P=S functionalities, resulted in ^{31}P chemical shift changes by up to 100 ppm as summarized in Table 1.[3-7] In rationalizing such results one of the guiding principles that has come through theoretical and experimental studies is the concept of electronegativity, *i.e.* that increase in electron density of an atomic nucleus enhances its shielding, resulting in an upfield chemical shift. However, excepting triesters (Table 1) the ^{31}P NMR chemical shifts for OP pesticides show upfield shifts when strong electronegative atoms or groups are attached, *i.e.* an inverse chemical shift trend which is contrary to what may have been expected.[2,8] Furthermore, the ^{31}P NMR chemical shifts for OP pesticides show upfield shifts when the OP is coordinated to transition metals.[3,4,8] Similarly, in studies of the

series of compounds **Ia-d** containing different X substituents on the *meta* and *para* positions of the phenyl moiety, it was found that electron withdrawing substituents lead to an upfield shift of the ^{31}P signal, pointing to a shielding effect on the P atom.[9]

However, contrary wise, in studies of the alkyl and aryl phosphinate ester series **IIa-c** Hoz, Buncel and co-workers[10b] found that electron-withdrawing substituents (X) induced downfield shifts in ^{31}P chemical shift, *i.e.* a normal dependence on the substituent effect. For all three sets, **IIa-c**, correlation of δ^{31}P with Hammett-Taft σ (or σ^o and σ^-) were correlated, however, σ^- value was most preferred over application to the alkyl and aryl phosphinates. The correlation between δ^{31}P and sign could be accounted for by considering the resonance structures **IIIa** and **IIIb** where **IIIb** results from donation of an electron pair on the phenoxy oxygen to a d orbital of the partially positive P atom in **III**.

IIIa   **IIIb**
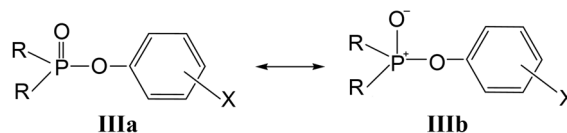
It was proposed in the case of the phosphinate ester series **IIa-c** that the electron-withdrawing substituents act to deplete the electron density on the aryl oxygen, thereby weakening a p_π-d_π bonding interaction between the aryl oxygen and phosphorus.[10c] The incidence of d_π-p_π bonding has also been invoked by other workers. Grabiak *et al*.[11] noted that an increase in the d_π-p_π bond back-donation effect was responsible for an increase in d-orbital occupation on phosphorus and a shift of the ^{31}P signal to higher field. This shift to higher field is accounted for by the increase in P=O bond order by stabilizing the major resonance structure **IVa** relative to **IVb** when electron-withdrawing groups (EWG)
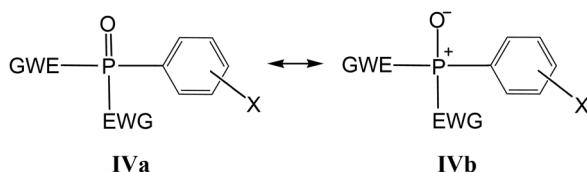

I (a-d)   **II (a-d)**

Y = F, Cl, OH, OEt   R^1 = R^2 = Me; R^1 = Me, R^2 = Ph; R^1 = R^2 = Ph

[a]On leave from the Department of Chemistry Education, Gyeongsang National University Jinju, Gyeongnam, 660-701, Korea
[b]Visiting Research Fellow from H.E.J. Research Institute of Chemistry, University of Karachi, Pakistan

are neighbouring the phosphorus atom.[11]
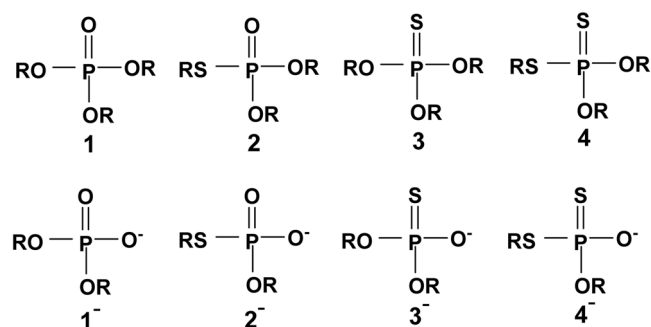

IVa   **IVb**

A number of attempts to develop a unified theoretical foundation for ^{31}P chemical shifts have been made. Factors such as electronegativity differences, π-electron overlaps (p_π-d_π bonding) and σ-bond angles between phosphorus and the bonded atoms or groups have been identified as contributions to the origin of the chemical shifts.[10] Ziegler *et al.*[12] have calculated ^{31}P NMR theoretical chemical shifts for phosphines using the Amsterdam Density Functional (ADF) package.[13] The results for calculated chemical shifts and the components of the chemical shifts tensor are in good agreement with the available experimental data. Also, the results of ADF calculations show that the ^{31}P NMR chemical shifts are dominated by the paramagnetic contribution.[10(a),12] Although numerous ^{31}P NMR experimental and theoretical studies of OP pesticides and their metal complexes have been reported, the systematic rationalization of the chemical shifts has been made a little. In order to determine the origin for the relative chemical shifts in the ^{31}P NMR spectra of OP esters, we have performed calculations of ^{31}P NMR chemical shifts for a family of organophosphorus esters **1** to **4** and their anions **1**$^-$ to **4**$^-$ (Scheme 1) and PA$^-$ (**5**) and its metal complexes such as Ag$^+$ and Hg^{2+}, and present the results herein.

5
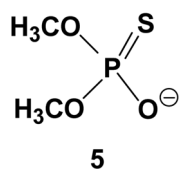
Theoretical Study: Methodology

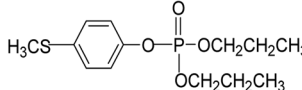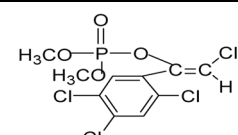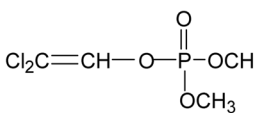As the experimental field of multinuclear NMR increases in importance, the theoretical calculation of NMR properties are reques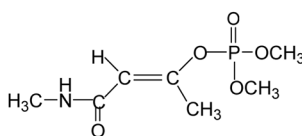ted to be provide the ability to wide variety of systems. Semi-empirical theories are only reliable for analogues of already understood systems, while traditional *ab initio* methods are constrained by the expense involved in treating electron correlation adequately. Density functional theory (DFT) provides a third path between these two methods and is now often the method of choice for investigating organic and inorganic systems, especially those containing metals. In this work calculations for ^{31}P NMR chemical shifts have been carried out using the Gaussian 98 package.[14] Structures have been fully optimized at the DFT of Becke's 3-parameter hybrid method using the correlation function of Lee, Yang, and Parr (B3LYP)[15] at 6-31G(d) level. Calculations of absolute shielding constants have been performed using the gauge-including atomic orbitals (GIAO) perturbation method[16] with HF and MP2 methods at 6-311+G(2d, p) level. For the larger molecules only the HF method was used to compute absolute shielding constants. Theoretical ^{31}P chemical shifts were calculated using absolute shielding constants and reference to H$_3$PO$_4$ ($\delta = 0.0$) Also, the ADF packages[13,17] were used to the complement some of the Gaussian calculations.
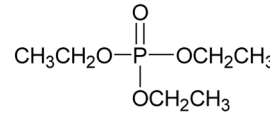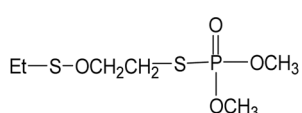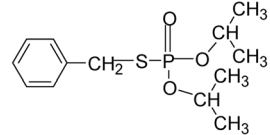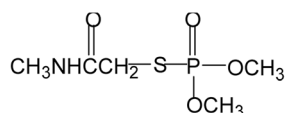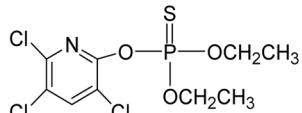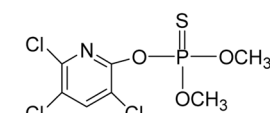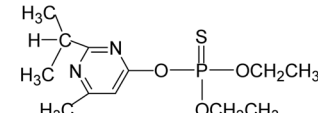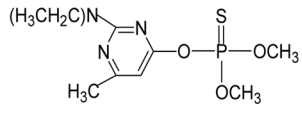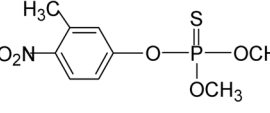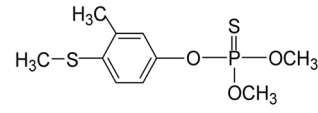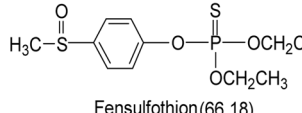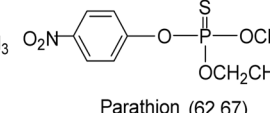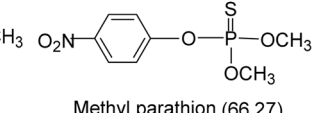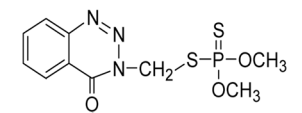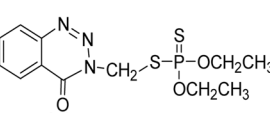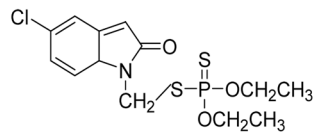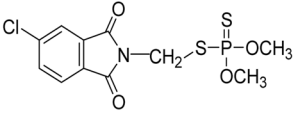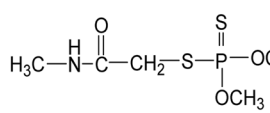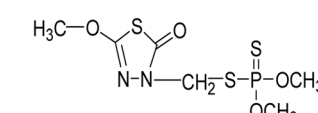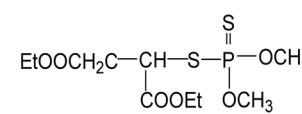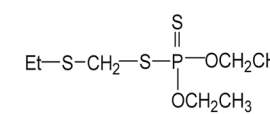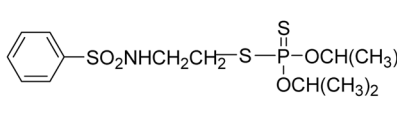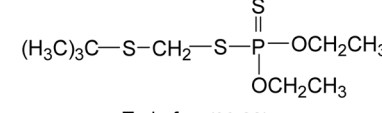
Results and Discussion

Experimental values of P chemical shifts amongst real chemicals classified by different functionalites are listed in Table 1. The first column of Table 1 is corresponds with the Scheme 1. The last column, 4 as shown in Table 1 is average values of experimental chemical shifts and compared with reference chemical shifts in which is H$_3$PO$_4$ here. The theoretical GIAO calculation of absolute nuclear shieldings (in ppm) of organophosphorus esters and organophosphorus ester anions has been performed using by both Gaussian and ADF commercial packages. Each structure, 1, 2, 3 and 4, and 1$^-$, 2$^-$, 3$^-$ and 4$^-$ in Tables 2 and 3 corresponds to the same as shown is Table 1 respectively. The Gaussian calculation results for the absolute chemical shifts are listed in Tables 2 and 3 respectively. The calculated relative chemical shifts are in good agreements with those of experimental values. We tried both methods of SCF and Moller Plesset Perturbation (MP2). However, the results from MP2 did not improve significantly. Also, we are reporting the calculations results of P, O and S charges. ^{31}P chemical shifts have been calculated using the absolute shielding constants and with reference to H$_3$PO$_4$ ($\delta = 0.0$). Computed ^{31}P NMR chemical shifts for organophosphorus esters are in good agreement with those of experimental mean values (see Tables 1 and 2). Atomic net charges for phosphorus and organophosphorus ester anions shifts in the order **4 < 3 < 2 < 1** (Table 1). However, calculated ^{31}P NMR chemical shifts for organophosphorus esters and their anions decrease in the order **4 > 3 > 2 > 1**. The differential electronic structure including the bond order and charge localization of the P=O and P=S bond are discussed in detail elsewhere,[18] so we do not discuss it in the present work. However, the relative bond order and charge localization show to vary the structure of phosphorus compounds changes. Also, the origin of
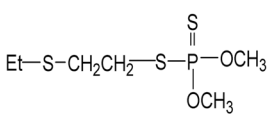

Scheme 1. Organophosphorus oxo and thio esters **1-4** and their anions **1$^-$-4$^-$**.

Table 1. ^{31}P NMR chemical shifts for various types of organophosphorus esters

	Structures (δ, ppm)	Average (δ, ppm)
1	Propaphos (-5.28) Tetrachlorvinphos (-4.05) Dichlorvos (-3.56) Monocrotophos (-5.03) Triethyl phosphate (-0.6)	−3.70 (±1.67)[a]
2	Oxydemeton-methyl (30.14) Iprobenfos (24.01) Omethoate (31.17)	28.11 (±2.90)[a]
3	Chloropyrifos (61.53) Chloropyrifos-methyl (65.77) Diazinon (60.98) Pirimifos-methyl (64.11) Fenirothion (66.31) Fenthion (67.39) Fensulfothion (66.18) Parathion (62.67) Methyl parathion (66.27)	64.58 (±2.21)[a]
4	Azinphos-methyl (96.50) Azinphos-ethyl (91.23) Phosalone (91.75) Phosmet (95.59) Mimethoate (99.38) Methidathion (94.78) Malathion (96.27) Thiometon (99.65) Phorate (93.51) Bensulide (90.76) Terbufos (93.22)	94.79 (±2.90)[a]

[a] Standard deviation

Table 2. GIAO calculation of absolute nuclear shieldings (in ppm), chemical shifts (δ, ppm) of ^{31}P and atomic net charges for organophosphorus esters

Structure	σ HF (δ)[a]	σ MP2 (δ)[a]	Charge (P, X(O or S))	
H_3PO_4	346.3 (0)	331.4 (0)		
1	345.2 (1.1)	327.9 (3.5)	1.655,	−0.659
2	308.4 (37.9)	293.5 (37.9)	1.479,	−0.616
3	261.1 (85.2)	245.7 (85.7)	1.389,	−0.490
4	228.0 (118.3)	214.6 (116.8)	0.793,	−0.433

[a]δ(mol) = σ(H_3PO_4) − σ(mol); relative to H_3PO_4 (δ = 0.0).

Table 3. GIAO calculation of absolute nuclear shieldings (in ppm), chemical shifts (δ, ppm) of ^{31}P and atomic net charges for organophosphorus ester anions

Structures	σHF (δ)[a]	MP2 (δ)[a]	Charge (P, X(O or S))	
H_3PO_4	346.3 (0)	331.4 (0)		
1⁻	339.6 (6.7)	324.4 (7.0)	0.980,	−0.605[b]
2⁻	319.4 (26.9)	309.7 (21.7)	0.668,	−0.538[b]
3⁻	271.2 (75.1)	259.3 (72.1)	0.702,	−0.728
4⁻	249.5 (96.8)	240.0 (91.4)	0.413,	−0.681

[a]δ(mol) = σ(H_3PO_4) − σ(mol); relative to H_3PO_4 (δ = 0.0). [b]average value of two non equivalent O atoms.

the differential reactivity of those compounds has not yet been provided. The d_π-p_π back-donation effect at the P=O double bond is a generally accepted theory in many respects. One can expect larger d orbital density of the P atom in P=O compounds than that of the P atom in P=S compounds. In order to confirm the d_π-p_π back-donation effect, we have calculated phosphorus d orbital density for organophosphorus esters and organophosphorus anions. Plots of absolute shielding constant versus d orbital density of the P atom in organophosphorus esters and organophosphorus anions are shown in Figures 1 and 2 respectively. Absolute shielding constants were in good agreement with the phosphorus d orbital density for organophosphorus esters and organophosphorus anions as shown in Figures 1 and 2. Therefore, d orbital density (population) of ^{31}P is larger with P=O than P=S. Increases in d orbital density translate into increases in paramagnetic property, like the anisotropy effect. The result of the higher d orbital density on P of P=O means to shift an upfield chemical shift (δ) for P=O relative to P=S. These results are explained by greater paramagnetic contribution in ^{31}P NMR chemical shifts than diamagnetic
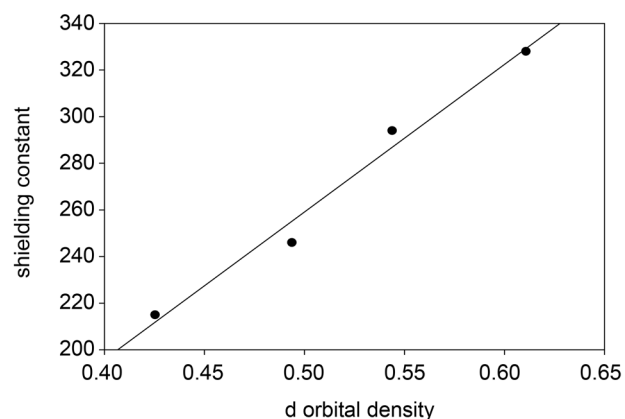
Figure 1. Absolute shielding constant versus d-orbital density for organophosphorus esters.
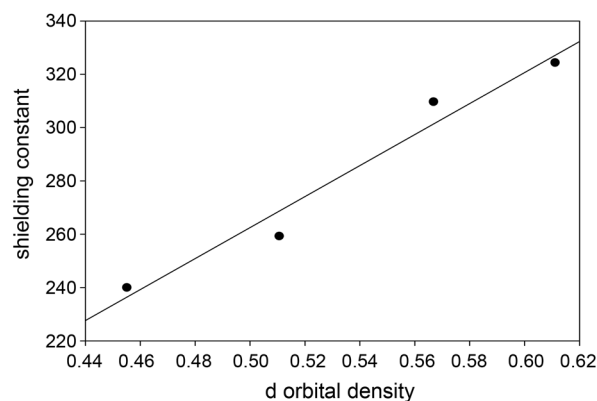
Figure 2. Plot of absolute shielding constant versus d-orbital density for organophosphorus esters anions.

properties.[10,12] Diamagnetic and paramagnetic contributions to chemical shift are described in the following equations (δ):[19,20]

$$\delta = \sigma_{\text{phosphoric acid}} - \sigma_{\text{compound}} = \delta^d + \delta^p \qquad (1)$$

$$\delta^d = \sigma^d_{\text{phosphoric acid}} - \sigma^d_{\text{compound}} \qquad (2)$$

$$\delta^p = \sigma^p_{\text{phosphoric acid}} - \sigma^p_{\text{compound}} \qquad (3)$$

The diamagnetic components (δ^d) to chemical shift does not affect ^{31}P NMR chemical shift as much as the paramagnetic component, δ^p (see Table 4),[12] thus the paramagnetic contribution is dominant.[12] In order to have a better

Table 4. The ADF calculation results of chemical shifts and individual paramagnetic and diamagnetic tensor components for organophosphorus esters[a]

Molecules	b^(1)ᵖ	μ^(1)ᵖ	s^(1)ᵖ	gaugeᵖ	TPTᵖ	coreᵈ	balanceᵈ	TDTᵈ	σLDA (δ[b])
H_3PO_4	−188.2	−514.86	118.62	−3.41	−587.87	903.35	58.29	961.64	373.77 (0)
1	−182.85	−534.88	118.43	−0.752	−600.06	903.35	59.53	962.88	362.82 (10.95)
2	−156.21	−573.25	105.08	−1.06	−625.44	903.36	60.66	964.01	338.57 (35.21)
3	−135.51	−608.94	76.52	−1.502	−669.43	903.59	60.24	963.59	294.16 (79.61)
4	−123.65	−651.04	78.86	−1.949	−697.78	903.35	61.27	964.63	266.85 (107.9)

[a]All numbers are in ppm. Superscript p and d indicate paramagnetic and diamagnetic components, respectively. [b]Chemical shifts are given with reference to H_3PO_4 (δ = 0.0). TPT = total paramagnetic tensor. TDT = total diamagnetic tensor.

understanding of diamagnetic and paramagnetic contributions for the P chemical shifts, we performed individual paramagnetic and diamagnetic tensor component calculations using ADF package. The total diamagnetic and paramagnetic contributions are break down to total six individual tensors. Defining the NMR shielding tensor is the first step to calculate NMR absolute chemical shifts. In the absence of electrons, the magnetic field felt at the nucleus is the same as the external magnetic field. In the presence of electrons the magnetic field induces electronic currents that create their own magnetic fields. As mentioned above the magnetic field at the nucleus may be different to the external magnetic field. Paramagnetic currents reinforce the external field and thus deshield the nucleus. Diamagnetic currents counter the external field and thus shield the nucleus.

The magnetic field at the nucleus and the external magnetic field can be related by 3X3 NMR shielding tensor.[12b] In solution, because the molecules are rapidly tumbling, only the trace of the tensor gives the NMR isotropic shielding constant. Calculating the NMR shielding tensor starts with defining the Hamiltonian. It could be expressed for the energy of a system in terms nuclear magnetic moment and the external magnetic field B, then the NMR shielding tensor can be determined from the Kohn-Sham energy using a relativistic Hamiltonian h. The Pauli Hamiltonaian or the Zeroth Order Regular Approximation (ZORA) can be applied to the given system. Given a Hamiltonian, the magnetic field that acts on the electrons, originates from both the external magnetic field and the nucleus magnetic field. The next logical step is to introduce the molecular orbital and basis functions. With including the spin orbital coupling, the α and β spins get mixed up. So the MOs have the complex coefficients and basis functions. Because the magnetic potential A is used in the density functional formalism instead of the magnetic field B in the Hamiltonian, we get gauge-invariance problems. From a consequence of this process, we can get different values of energy, NMR shieldings, and other properties for the condition of the moving molecules. To solve this problem we use gauge-including atomic orbitals (GIAO) as our basis functions. Also, the NMR tensor can be partitioned into three parts. For the Pauli

formalism, the NMR shielding tensor can be partitioned into the three parts of paramagnetic, diamagnetic and Fermi-contact. For the ZORA formalism, the NMR shielding tensor expression can be partitioned into the tree parts of paramagnetic, diamagnetic and spin-orbit. The paramagnetic tensor can be further break down to four tensor components (please see Table 4); $b^{(1)p}$ is the first-order change in the core-orthogonalization coefficients, $\mu^{(1)p}$ is the first-order change in the MO coefficients, $s^{(1)p}$ is the first-order change in the overlap matrix and gauge components. The diamagnetic tensor can be break down to tow parts as core part and balance part respectively. The calculations results on individual tensors are shown in Table 4. Also, the final calculated chemical shifts are compared with Table 1. The theoretical derivations and definitions of these tensors are explained in details at the pioneering work by Ziegler.[12] The diamagnetic components (δ^d) to chemical shift are reported to be not affected to the ^{31}P NMR chemical shift as much as the paramagnetic component, δ^p (see Table 4),[12] thus the paramagnetic contribution is dominant.[12] As pointed out by Chesnut, s and p orbital contributions lead to bond shortening, while d and f orbital contributions tend to expand and destabilize bonds.[21] Table 4 shows the individual paramagnetic and diamagnetic tensor components. These results are in good agreement between theoretical and experimental ^{31}P NMR chemical shifts for organophosphorus esters (see

Table 5. GIAO calculation of absolute nuclear shieldings (in ppm), chemical shift (δ, ppm) of ^{31}P, atomic net charges and experimental chemical shift (δ, ppm) for PA$^-$ and PA$^-$ with metal ions

PA and PA Complex	σHF (δ)[a]	σMP2 (δ)[a]	Charge[b] (P, S)	exp(δ)[c]
PA$^-$	271.3 (75.0)	259.4 (72.0)	0.703, −0.727	65.94
PA$^-$···Ag$^+$	276.3 (70.0)	258.5 (72.9)	0.702, −0.421	43.30
(PA$^-$)$_2$···Ag$^+$	286.5 (59.8)		0.486, −0.378	
PA$^-$···Hg^{2+}	290.1 (56.2)	273.3 (58.1)	0.688, −0.071	40.54
(PA$^-$)$_2$···Hg^{2+}	281.8 (64.5)		0.473, −0.379	
H$_3$PO$_4$	346.3 (0)	331.4		

[a]δ(mol) = σ(H$_3$PO$_4$) − σ(mol); relative to H$_3$PO$_4$ (δ = 0.0). [b]HF/6-311+g(d). [c]From reference 22.
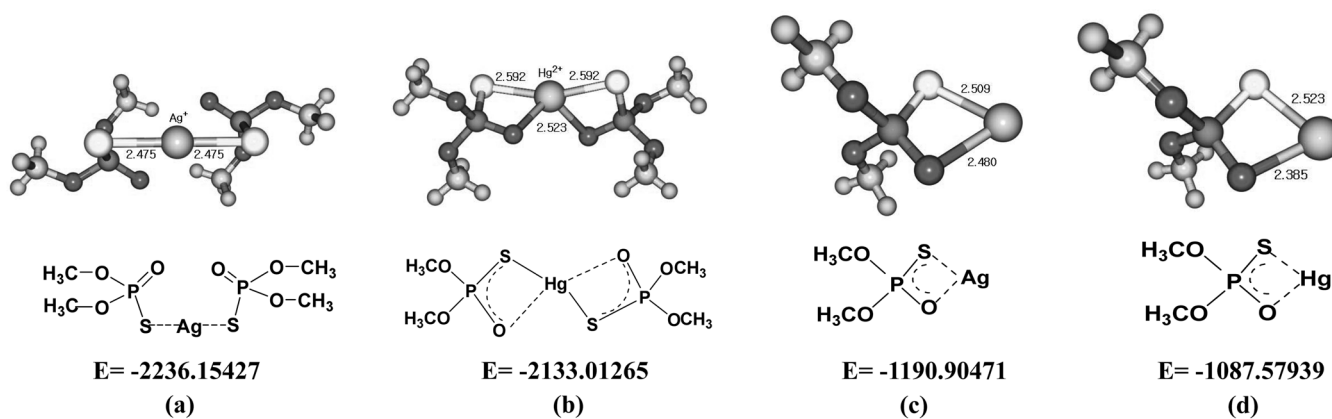

Figure 3. Theoretical optimized structures: (a) PA–Ag–PA, (b) PA–Hg–PA, (c) PA–Ag and (d) PA–Hg complexes. Energies here are hartree unit.

Table 6. ADF calculation of absolute nuclear shieldings (in ppm) and some structural parameters

PA and PA⁻···Metal	σLDA^a (δ)^b	Exp(δ)^c	Bond length (Å) and Bond angle (degree, °)	
PA⁻	309.63 (64.14)	*ca.* 65		
S-metallated PA⁻···Ag⁺ (Figure 5a)	320.91(52.86)	*ca.* 40	S···Ag	2.5641 (Å)
			P=O···Ag	3.0047(Å)
			=O–P–S	121.56 (°)
O-metallated PA⁻···Ag⁺ (Figure 5b)	305.35 (68.42)	*ca.* 43	S···Ag	2.4654(Å)
			P=O···Ag	2.3551(Å)
			=O–P–S	116.172(°)
(PA⁻)₂···Ag⁺ (similar to Figure 3a)	316.16 (57.61)			
	311.01(62.76)			
PA···Hg²⁺ (similar to Figure 5a)	316.88 (57)	*ca.* 40	S···Hg	2.5641(Å)
			P=O···Hg	3.208(Å)
			=O–P–S	121.6(°)
(PA)₂···Hg (similar to Figure 3b:)	306.63 (67.14)			
	304.21 (69.16)			
H₃PO₄	373.77			

$^a\sigma$LDA: total shielding components. $^b\delta$(mol) = σ(H₃PO₄) − σ(mol); relative to H₃PO₄ (δ = 0.0). ^{c}From reference 24.

Tables 1 and 4). The total shielding components σLDA are dominated by the large positive diamagnetic components core^d and balance^d whereas the paramagnetic components b^(1)^p and μ^(1)^p are negative. Total diamagnetic tensor (TDT) is constant whereas the total paramagnetic tensor (TPT) indicates a large change for the different structures of organophosphorus esters. ^{31}P chemical shifts are dominated by paramagnetic contribution whereas diamagnetic components will not contribute much to the ^{31}P chemical shift since diamagnetic shielding largely comes from constant core terms.[5,12]

Metal ion effects on ^{31}P chemical shift of PA⁻. Results of GIAO calculations of absolute nuclear shieldings (in ppm) and atomic net charges for bidentate PA⁻ and PA⁻ with metal ions are given in Tables 5. The geometry and charge density of the bidentate PA⁻···Ag⁺ (Hg²⁺) and (PA⁻)₂···Ag⁺ (Hg²⁺) complexes in the gas phase are shown in Figure 3. Examination of the calculated ^{31}P NMR shifts and the geometries of PA⁻-metal cation complexes leads to the following suggestions: the metal cation complexation decreases the mag-
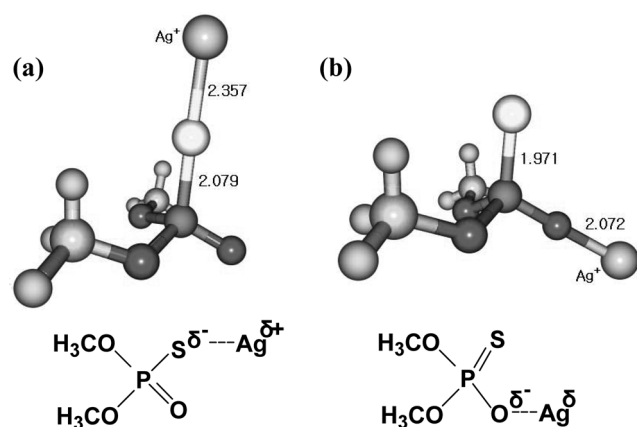

Figure 5. Theoretical optimized structures of PA–Ag by ADF output. S-metallated PA⁻···Ag⁺ and (b) O-metallated PA⁻···Ag⁺ (PA⁻···Hg²⁺ complex has similar structure).

nitude of the chemical shifts (more upfield), and the cation prefers to bind to the sulfur atom rather than the oxygen atom. Tight binding of the metal cation with the S atom can be rationalized by taking the difference of atomic radii between S and O atoms into account. The atomic radii of sulfur and oxygen atoms are 1.04 Å and 0.66 Å, respectively. However, the difference of bond length of S···Ag and O···Ag is only 0.03 Å, showing tight binding with sulfur atom in the complex. As a consequence of the above comparison with experimental and theoretical results, the ^{31}P NMR chemical shifts of PA⁻···metal ion complexes are observed higher upfield (26-28 ppm[22]).

Results of ADF calculations of absolute nuclear shieldings (in ppm) and structure values are given in Table 6 using LDA correation functions and TZP basis set. The Gaussian B3LYP calculation results indicate that both Ag⁺ and Hg²⁺ complexes are optimized to the complex structures of Figure 3 (a, b, c and d). Partially energy optimized structures with restriction of linear configuration for S-metallated PA···Ag⁺ and O-metallated PA···Ag⁺ complexes are given in Figure 4(4a-b). However, in the ADF calculations, the optimized structures S-metallated PA⁻···Ag⁺ structure has shown as the actual bond energy was −2.894793 a.u. whereas the O-metallated PA⁻···Ag⁺ structure bond energy was −2.85151 a.u. The S-metallated structure has significantly lower energy than the O-metallated structure. The PA⁻ with bound

Figure 4. Theoretically optimized structures: (a) S-metallated PA⁻ ···Ag⁺ and (b) O-metallated PA⁻···Ag⁺ (PA⁻···Hg²⁺ complex has similar structure).

metal ion is in accordance with the hard-soft acid-base (HSAB) principle.[23] Also, the chemical shifts for both Ag^+ and Hg^{2+} S-metallated complexes has shown to be in good agreement with the experimental values.

Figure 5 shows the cartoon model of ADF results on S-metallated $PA^- \cdots Ag^+$ and O-metallated $PA^- \cdots Ag^+$ ($PA^- \cdots Hg^{2+}$ complex has similar structure).

Conclusions

In this work the electronic influence of constituents at phosphorus atoms on ^{31}P NMR chemical shifts has been examined theoretically. The major contribution of ^{31}P NMR chemical shifts derives from the total paramagnetic tensor and the variation of d orbital population on the P atom by d_π-p_π bond back-donation.

References

1. (a) Balakrishnan, V. K.; Han, X.; vanLoon, G. W.; Dust, J. M.; Toullec, J.; Buncel, E. *Langmuir* **2004**, *20*, 6586. (b) Balakrishnan, V. K.; Dust, J. M.; vanLoon, G. W.; Buncel, E. *Can. J. Chem.* **2001**, *79*, 157. (c) Eneji, I. S.; vanLoon, G. W.; Buncel, E. *J. Agric. Food Chem.* **2002**, *50*, 5634. (d) Balakrishnan, V. K.; Buncel, E.; vanLoon, G. W.; *Environ. Sci. Tecnol.* **2005**, *39*, 5824. (e) Lumbiny, B. J.; Adhikary, K. K.; Lee, B.-S.; Lee, H. W. *Bull. Korean Chem. Soc.* **2008**, *29*, 1773.

2. Kireev, A. F.; Rybal'chenko, I. V.; Khamidi, B. A.; Kholstov, V. I. *J. Anal. Chem.* **2001**, *56*, 421.

3. Mortimer, R. D.; Dawson, B. A. *J. Agric. Food Chem.* **1991**, *39*, 911.

4. Mahajna, M.; Quistad, G. B.; Casida, J. E. *Chem. Res. Toxicol.* **1996**, *9*, 1202.

5. Miyata, Y.; Ando, H. *Jpn. J. Toxicol. Environ. Health* **1994**, *40*(1), 49.

6. Greenhalgh, R. *et al. J. Agric. Food Chem.* **1983**, *31*, 710.

7. Kirk, K.; Kuchel, P. W. *Biochemistry* **1988**, *27*, 8803.

8. Pehkonen, S. O.; Judeh, Z. M. A. *Environ. Sci. Technol.* **2005**, *39*, 2586.

9. Hesse, M.; Meier, H.; Zeeh, B. *Spectroscopy Methods in Organic Chemistry*, Thieme Foundations of Organic Chemistry Series; Enders, D., Noyori, R., Trost, B. M., Eds.; G. T. Verlag: Berlin, Germany, 1997.

10. (a) *Phosphorus-31 NMR*; Gorenstein, D. G., Ed.; Academic Press: New York, 1984; Ch. 1. (b) Hoz, S.; Dunn, E. J.; Buncel, E.; Bannard, R. A. B.; Purdon, J. G. *Phosphorus and Sulfur* **1985**, *24*, 321. (c) Dunn, E. J.; Purdon, J. G.; Bannard, R. A. B.; Albright, K.; Buncel, E. *Can. J. Chem.* **1988**, *66*, 3137.

11. Grabiak, R. C.; Miles, J. A.; Schwenzer, G. M. *Phosphorus Sulfur* **1980**, *9*, 197.

12. (a) Ruiz-Morales, Y.; Ziegler, T. *J. Phys. Chem. A* **1998**, *102*, 3970. G. Schreckenbach and T. Ziegler, J.Phys. Chem. 99 (1995) 606. (b) Schreckenbach, G.; Ziegler, T. *Int. J. Quantum Chem.* **1997**, *61*, 899.

13. (a) te Velde, G.; Bickelhaupt, F. M.; Baerends, E. J.; Fonseca Guerra, C.; van Gisbergen, S. J. A.; Snijders, J. G.; Ziegler, T. *J. Comp. Chem.* **2001**, *22*, 931. (b) te Velde, G. *Amsterdam Density Functional (ADF), User Guide*, Release 1.1.3; Department of Theoretical Chemistry, Free University: Amsterdam, The Netherlands, 1994.

14. Frisch, M. J.; Trucks, G. W.; Schlegel, H. B.; Scuseria, G. E.; Robb, M. A.; Cheeseman, J. R.; Zakrzewski, V. G.; Montgomery, J. A., Jr.; Stratmann, F. E.; Burant, J. C.; Dapprich, S.; Millam, J. M.; Daniels, A. D.; Kudin, K. N.; Strain, M. C.; Farkas, O.; Tomasi, J.; Barone, V.; Cossi, M.; Cammi, R.; Mennucci, B.; Pomelli, C.; Adame, C.; Clifford, S.; Ochterski, J.; Petersson, G. A.; Ayala, P. Y.; Cui, Q.; Morokuma, K.; Malick, D. K.; Rabuck, A. D.; Raghavachari, K.; Foresman, J. B.; Cioslowski, J.; Ortiz, J. V.; Stefanov, B. B.; Liu, G.; Liashenko, A.; Piskorz, P.; Komaromi, I.; Gomperts, R.; Martin, R. L.; Fox, D. J.; Keith, T.; Al-Laham, M. A.; Peng, C. Y.; Nanayakkara, A.; Gonzalez, C.; Challacombe, M.; Gill, P. M. W.; Johnson, B. G.; Chen, W.; Wong, M. W.; Andres, J. L.; Head-Gordon, M.; Replogle, E. S.; Pople, J. A. *Gaussian 98*, Revision A.7.; Gaussian, Inc.: Pittsburgh, PA, 1998.

15. (a) Becke, A. D. *J. Chem. Phys.* **1992**, *98*, 5648. (b) Lee, C.; Yang, W.; Parr, R. G. *Phys. Rev. B* **1988**, *37*, 785. (b) Lee, T. K.; Koo, Y.-M.; Kim, J.-S.; Jung, D. W.; Jung, K.-W. *Bull. Korean Chem. Soc.* **2008**, *29*, 725.

16. Ruud, K.; Helgaker, T.; Bak, K. L.; Jørgensen, P.; Jensen, H. J. A. *J. Chem. Phys.* **1993**, *99*, 3847.

17. Baerends, E. J.; Ellis, D. E.; Ros, P. *Chem. Phys.* **1973**, *2*, 41.

18. (a) Frey, P. A.; Sammons, R. D. *Science* **1985**, *228*, 541. (b) Schmidt, M. W.; Gordon, M. S. *J. Am. Chem. Soc.* **1985**, *107*, 1922.

19. Pople, J. A.; Schneider, W. G.; Bernstein, H. J. *High Resolution Nuclear Magnetic Resonance*; McGraw-Hill: New York, 1959.

20. Prado, F. R.; Geissner-Prettre, C.; Pullman, B.; Daudey, J.-P. *J. Am. Chem. Soc.* **1979**, *101*, 1737.

21. Chesnut, L. D.; Quin, L. D. *Tetrahedron* **2005**, *61*, 12343.

22. Koo, I. S. unpublished results.

23. (a) Pearson, R. G. *J. Am. Chem. Soc.* **1963**, *85*, 3533. (b) Pearson, R. G. *Science* **1966**, *151*, 172.